NeuroImage: Clinical 19 (2018) 516–526

Contents lists available at ScienceDirect

NeuroImage: Clinical

journal homepage: www.elsevier.com/locate/ynicl

Callosal circularity as an early marker for Alzheimer's disease

Jeroen Van Schependom[a,b,*], Ellis Niemantsverdriet[d], Dirk Smeets[c], Sebastiaan Engelborghs[d,e]

[a] Vrije Universiteit Brussel, Center for Neurosciences, Laarbeeklaan 103, 1090 Brussels, Belgium
[b] Radiology, Universitair Ziekenhuis Brussel, Laarbeeklaan 101, 1090 Brussels, Belgium
[c] Icometrix NV, Kolonel Begaultlaan 1b/12, 3012 Leuven, Belgium
[d] Reference Center for Biological Markers of Dementia (BIODEM), University of Antwerp, Universiteitsplein 1, 2610 Antwerpen, Belgium
[e] Department of Neurology and Memory Clinic, Hospital Network Antwerp (ZNA) Middelheim and Hoge Beuken, 2660 Antwerpen, Belgium

ARTICLE INFO

Keywords:
Corpus callosum
Thickness profile
Biomarker
Mild cognitive impairment
Subjective cognitive decline, Alzheimer's disease
Normal ageing

ABSTRACT

Background: Although brain atrophy is considered to be a downstream marker of Alzheimer's disease (AD), subtle changes may allow to identify healthy subjects at risk of developing AD. As the ability to select at-risk persons is considered to be important to assess the efficacy of drugs and as MRI is a widely available imaging technique we have recently developed a reliable segmentation algorithm for the corpus callosum (CC). Callosal atrophy within AD has been hypothesized to reflect both myelin breakdown and Wallerian degeneration.

Methods: We applied our fully automated segmentation and feature extraction algorithm to two datasets: the OASIS database consisting of 316 healthy controls (HC) and 100 patients affected by either mild cognitive impairment (MCI) or Alzheimer's disease dementia (ADD) and a second database that was collected at the Memory Clinic of Hospital Network Antwerp and consists of 181 subjects, including healthy controls, subjects with subjective cognitive decline (SCD), MCI, and ADD. All subjects underwent (among others) neuropsychological testing including the Mini-Mental State Examination (MMSE). The extracted features were the callosal area (CCA), the circularity (CIR), the corpus callosum index (CCI) and the thickness profile.

Results: CIR and CCI differed significantly between most groups. Furthermore, CIR allowed us to discriminate between SCD and HC with an accuracy of 77%. The more detailed callosal thickness profile provided little added value towards the discrimination of the different AD stages. The largest effect of normal ageing on callosal thickness was found in the frontal callosal midbody.

Conclusions: To the best of our knowledge, this is the first study investigating changes in corpus callosum morphometry in normal ageing and AD by exploring both summarizing features (CCA, CIR and CCI) and the complete CC thickness profile in two independent cohorts using a completely automated algorithm. We showed that callosal circularity allows to discriminate between an important subgroup of the early AD spectrum (SCD) and age and sex matched healthy controls.

1. Introduction

Volumetric magnetic resonance imaging (MRI) is of increasing importance in the follow-up of patients with mild cognitive impairment (MCI) or Alzheimer's disease (AD) (Filippi et al., 2012), with most attention being devoted to atrophy of the medial temporal lobe (MTL), hippocampus or entorhinal cortex. Although atrophy in these latter structures is considered to be a downstream topographical biomarker of AD with a limited value for early (preclinical) AD diagnosis (Dubois et al., 2014), it may provide a tool to follow up AD patients (Frisoni et al., 2010).

Whereas most studies report a high intra-class correlation coefficient (ICC) between automated and manual segmentation of the hippocampi, e.g. (Plassard et al., 2017; Zandifar et al., 2017), others report a low ICC (Akudjedu et al., 2018). Yet, segmentation of the entorhinal cortex often requires manual segmentation due to its inter subject variability, relatively small size and low contrast with surrounding structures. Although being time consuming, manual segmentation approaches have been widely used and are even a standard approach by experts in neuroanatomy (Boccardi et al., 2011). However, the number of large-scale studies is limited. Although semi-automated techniques are less time consuming, a priori information such as user-defined landmarks are needed, which also limits their usefulness for large clinical studies (Kennedy et al., 2010). To save time and costs,

* Corresponding author at: Vrije Universiteit Brussel, Pleinlaan 2, 1050 Brussels, Belgium.
E-mail addresses: Jeroen.Van.Schependom@vub.be (J. Van Schependom), Ellis.Niemantsverdriet@uantwerpen.be (E. Niemantsverdriet), Dirk.Smeets@icometrix.com (D. Smeets), Sebastiaan.Engelborghs@uantwerpen.be (S. Engelborghs).

https://doi.org/10.1016/j.nicl.2018.05.018
Received 5 December 2017; Received in revised form 10 May 2018; Accepted 13 May 2018
Available online 19 May 2018

automated methods have been proposed, which can be used in larger study populations and can be reproduced more easily.

Sensitive and reliable markers are needed to monitor disease progression or therapy response. As the whole-brain atrophy rate has been estimated at 1.4–2.2% in AD as compared to 0.7% in age-matched controls (Frisoni et al., 2010), it has been suggested as a marker to follow up AD patients. Yet, by assessing whole-brain atrophy, a lot of specificity is lost.

Therefore, an alternative MRI marker could be atrophy of the corpus callosum (CC) (Di Paola et al., 2010a, 2010b; Frederiksen et al., 2011; Hampel et al., 2002, 1998; Lyoo et al., 1997; Ortiz Alonso et al., 2000; Teipel et al., 2002, 1999, 1998; Thompson et al., 1998; Van Schependom et al., 2017; Wang et al., 2006; Yamauchi et al., 2000; Zhu et al., 2012). While callosal atrophy has been shown in AD and has been hypothesized to originate from myelin breakdown in the anterior CC regions and from Wallerian degeneration in posterior regions (Di Paola et al., 2010a, 2010b), both the affected CC region and the timing at which callosal atrophy can be observed are under debate. While some studies found differences in the posterior regions in early onset AD (Yamauchi et al., 2000), MCI patients (Wang et al., 2006), and mild AD dementia (ADD) patients (Frederiksen et al., 2011; Hampel et al., 2002; Lyoo et al., 1997; Wang and Su, 2006), others observed differences in the anterior regions in MCI (Zhu et al., 2012) and moderate ADD (Ortiz Alonso et al., 2000). Only one study assessed severe ADD patients and found differences in both anterior and posterior regions (Di Paola et al., 2010a, 2010b).

Apart from the CC area, one study found differences in circularity (ratio of the area to the perimeter) already in MCI patients (Ardekani et al., 2014) suggesting that morphological CC features may be more sensitive to disease specific changes than plain area.

As the CC can be automatically and reliably extracted from 3D T1 MR images (even in neurodegenerative diseases (Van Schependom et al., 2016)) and likely provides more detailed information than whole-brain atrophy, we aim at assessing its value in AD in two independent cohorts. The first cohort is the OASIS database, which contains a large number of subjects (100 ADD patients, 316 healthy controls). The second one is a monocentric cohort, collected at UAntwerp, covering the entire AD continuum. As a reference, we will also assess the effect of normal ageing in both cohorts.

Next to assessing overall features (area - CCA, circularity - CIR and CC index - CCI) or applying an artificial division of the CC into different sub regions, we will also calculate a thickness profile of equidistantly sampled streamlines along the CC midline. This method ensures non-crossing streamlines orthogonal to the boundaries and provides a ‘natural’ division of the CC while bypassing inherent problems that arise when trying to divide the CC in different regional areas (Adamson et al., 2011; Luders et al., 2007; Tomaiuolo et al., 2007).

2. Materials and methods

2.1. Study population 1: OASIS cohort

The OASIS database consists of 416 subjects aged 18–96. For each subject, 3 or 4 individual T1-weighted MRI scans obtained in single-scan sessions were included. The scans were acquired on a 1.5-T Vision scanner (Siemens). All subjects were right-handed.

Control subjects under the age of 60 were questioned about their medical histories and use of psychoactive drugs. For subjects older than 60 years, a global Clinical Dementia Rating (CDR, (Morris, 1993)) score (based on a collateral source and subject interview) was recorded. Furthermore, it is outlined by Markus et al. that *subjects with alternative primary causes of dementia* (e.g. *vascular dementia*, *primary progressive aphasia*), *active neurological or psychiatric illness* (e.g. *major depression*), *serious head injury*, *history of clinically meaningful stroke*, *and use of psychoactive drugs were excluded*, *together with subjects with gross anatomical abnormalities evident in their MR images* (e.g. *large lesions*, *tumors*) (Marcus et al., 2007).

Out of the 416 available subjects, 70 subjects had been diagnosed with MCI (“very mild AD”, according to the Clinical Dementia Rating (Morris, 1993), CDR = 0.5) while 28 subjects have been diagnosed with mild Alzheimer's Disease Dementia (mADD, CDR = 1) (Morris et al., 2001). Only the first of the 3–4 available MR T1-weighted scans was used for this analysis, although no differences are expected when one would use the other scans thanks to the high inter scan reliability (Van Schependom et al., 2016). For more information on this dataset, cf. (Marcus et al., 2007).

As the CC is suspected to be larger in females than in males (after correcting for intracranial volume) (Ardekani et al., 2013), we matched subgroups from the OASIS database to the clinical populations. Matching was performed on sex and age. Additional data on the subjects included in the OASIS database were sex, age, education, socio-economic status (SES, (Rubin et al., 1998)) and the Mini-Mental State Examination (MMSE) which is a widely used screening instrument for dementia (Folstein et al., 1975; Rubin et al., 1998).

2.2. Study population 2: UAntwerp cohort

The second database was collected at the Memory Clinic of Hospital Network Antwerp and consists of 181 subjects, including healthy controls, subjects with subjective cognitive decline (SCD), MCI, and ADD. All subjects underwent (among others) neuropsychological testing including MMSE.

A clinical diagnosis of dementia due to AD was made by applying the NIA-AA criteria (McKhann et al., 2011). A diagnosis of MCI due to AD was made by the NIA-AA criteria (Albert et al., 2011; Dubois et al., 2014; Jack et al., 2011; Sperling et al., 2011) i.e., (1) cognitive complaint, preferably corroborated by an informant; (2) objective cognitive impairment, quantified as performance of > 1.5 SD below the appropriate mean on the neuropsychological subtests; (3) largely normal general cognitive functioning; (4) essentially intact activities of daily living (basic and instrumental activities of daily living were determined by a clinical interview with the patient and an informant); and (5) not demented. The diagnosis of dementia or MCI due to AD was further corroborated either through AD biomarker analyses ($A\beta_{1-42}$, T-tau, and P-tau_{181}) in cerebrospinal fluid (CSF) according to the IWG-2 criteria (Dubois et al., 2014), based on in-house validated cut-off values (Van Der Mussele et al., 2014), and/or through hippocampal atrophy based on the Scheltens scale (Scheltens et al., 1992).

SCD patients were diagnosed by the Jessen's et al. criteria (Jessen et al., 2014), without an objective cognitive impairment, so all neuropsychological subtests having a z-score above -1.5 SD.

All control subjects underwent at least a cognitive screening test to rule out cognitive impairment. The inclusion criteria for cognitively healthy elderly were: (1) no neurological or psychiatric antecedents; (2) no organic disease involving the central nervous system following extensive clinical examination; and (3) no cognitive complaint or decline.

All subjects provided written informed consent and the study was approved by the ethics committee of University of Antwerp, Antwerp, Belgium.

2.3. Corpus callosum segmentation

The applied algorithm to segment the CC and to extract the different features has been extensively described and validated in both healthy controls and subjects affected with multiple sclerosis or AD (Van Schependom et al., 2016).

In short, our method first automatically extracts the Mid Sagittal Plane (MSP) maximising the symmetry between the two brain hemispheres. This MSP is resampled to voxels of $0.5 \times 0.5\,mm^2$. Next, a 3D affine registration between an MNI template and the patient's MRI allows to translate and rotate an average CC to its initial position within the MSP. In the optimisation step, the (interpolated) pixel intensities

are calculated along the normal of all edge points and compared to the observed pixel intensities in a training set. This allows every point on the edge of the current CC shape to be translated along this normal. Subsequently, the resulting shape is projected onto the eigenvectors calculated from the training set and the process is repeated until convergence. This active shape model allows the CC to adjust to the large inter-individual variety of CC shapes and leads to a highly reliable and reproducible extraction (and subsequent thickness profile calculation) of the CC.

2.4. Morphometric features

2.4.1. Corpus Callosum Area (CCA)

The CCA was calculated by applying Green's theorem on the resulting contour: This method has the advantage of fully exploiting the continuous nature of the edges obtained by the active shape model and bypasses the partial volume effects as it does not require every pixel to be classified as either CC or not CC. This results into slightly smaller CC areas than those found when using a pixelated method.

2.4.2. Circularity (CIR)

In (Ardekani et al., 2014), Ardekani et al. argue that CCA alone may not capture the effect of ventricular dilation and therefore suggested circularity as an appropriate measure to follow AD patients. Circularity is defined as $4\pi\frac{CCA}{p^2}$, with P being the perimeter calculated as the sum of the Cartesian distances between all subsequent points. CIR therefore reduces both when the CCA reduces or the perimeter increases. As CIR (in contrast to CCA) showed the ability to discriminate between MCI and mild ADD patients, Ardekani et al. concluded that it should be included in future studies [21].

2.4.3. Corpus Callosum Index (CCI)

In order to calculate the CCI, one needs to determine the greatest anterior-posterior diameter. The 3 line segments under consideration are those where this anterior-posterior line (or the normal constructed on its middle point crosses the corpus callosum (cf. Fig. 3 in (Yaldizli et al., 2013)). As this measure is sometimes used as an easy-to-calculate measure, we have included it for comparison reasons.

2.4.4. Thickness Profile Generation

The Corpus Callosum thickness profile generation was performed using Laplace's equation, based on (Adamson et al., 2011). First, a scalar field is calculated between the inferior and superior part of the CC that needs to be Laplacian (i.e. $\frac{\partial^2\varphi}{\partial x^2} + \frac{\partial^2\varphi}{\partial y^2} = 0$). The inferior and superior part can be easily separated by the use of the active shape model, that allows to reliably select equivalent points in different CCs.

Next, the midline is found as the line where the Laplacian field assumes the mean value of the two extremes imposed on the inferior and posterior edge. Finally, 50 equidistant points are calculated on this line and streamlines are calculated from this midline to both the inferior and superior edge. Similar to Adamson et al. (2014), we used the first-order Euler approximation to the gradient of the Laplacian field in order to construct the streamlines. The sum of the distances covered by these streamlines is the thickness at that point.

For a more extensive explanation and validation of the different algorithms, we refer to (Van Schependom et al., 2016).

2.4.5. Correction for ICV

In order to correct for the estimated intracranial volume (ICV), CCA was divided by ICV^(2/3) and CIR and thickness by ICV^(1/3) leading to dimensionless numbers.

2.5. Statistics

All subpopulations were carefully matched on age and sex (cf. Table 1). All univariate comparisons were performed using the non-parametric version of the *t*-test, the Wilcox rank test. The advantage of the latter is that it does not assume an underlying Gaussian distribution of variables. A p-value of 0.05 was considered significant for a single test. In order to address the multiple comparison problem, a strict Bonferroni procedure was applied within each group comparison, resulting in a p-value of $0.05/3 = 0.017$.

The corpus callosum thickness profile was compared on 50 equidistant points along the CC midline. These comparisons are not independent as the length of adjacent streamlines is obviously correlated. In order to estimate the true dimensionality of the data, we will perform a principal component analysis (PCA).

2.6. Ethics, consent, and permission

2.6.1. OASIS

All subjects included in the OASIS database (http://oasis-brains.org/) participated in accordance with guidelines of the Washington University Human Studies Committee. Approval for public sharing of the data was also specifically obtained (Marcus et al., 2007).

2.6.2. UAntwerp

All subjects provided written informed consent and the study was approved by the ethics committee of University of Antwerp, Antwerp, Belgium (16/2/18).

3. Results

3.1. Datasets

3.1.1. OASIS

The demographic and clinical characteristics from the different (matched) groups have been summarized in Table 1. The group of healthy controls included in Table 1 is matched with the combined group of both MCI and mild ADD subjects. Three different groups of healthy controls are selected to specifically match the MCI, mADD and the total cohort of AD (MCI + mADD) subjects.

3.1.2. UAntwerp dataset

After a manual quality check of the segmented corpora callosa, 42 healthy controls, 22 SCD subjects, 82 MCI subjects and 34 subjects diagnosed with ADD were retained. Out of these 34, 8 were classified as possible ADD and 26 were classified as probable ADD. For 15 out 34 ADD subjects, the clinical diagnosis could be complemented through a positive CSF biomarker profile, while for 7 others a positive neuroimaging biomarker profile complemented the clinical diagnosis.

Limiting the MCI group to the subgroup with a diagnosis supported by either imaging or CSF biomarkers resulted in a cohort of 53 subjects. As the MCI group was significantly older than both the HC and the ADD group, we excluded all MCI subjects older than 80 years, reducing the number of MCI subjects to 41. In this cohort, 21 MCI subjects were diagnosed with multi-domain amnestic MCI, 13 with single-domain amnestic MCI, 4 with single-domain non-amnestic MCI and 3 with multi-domain non-amnestic MCI. The MCI diagnosis was corroborated by a positive CSF biomarker profile in 24 cases and a positive neuroimaging biomarker profile in 17 cases.

As there were no significant differences between the MCI and ADD group based on age (p-value through a Wilcoxon's ranksum test > 0.05) nor sex (p-value of chi-squared test > 0.05), two cohorts of healthy controls were extracted. One to match the MCI/ADD group and one to match the SCD cohort (cf. Table 1). The results barely change when correcting for age (cf. Table S1).

3.2. Corpus Callosum features of neurodegeneration

The obtained results have been summarized in Table 2 for both

Table 1
Demographic and clinical characteristics of the different groups involved.

		Healthy controls				MCI	AD subjects		
							MCI	mADD	MCI + mADD
	Matched to	–	MCI	mADD	MCI + mADD	mADD	–	–	–
OASIS	N	316	85	81	80	67	69	28	97
	Sex (M/F)	119/197	35/50	24/57	32/48	29/38	31/38	9/19	40/57
	Sex (% F)	62	59	70	60	57	55	68	59
	Age	45.0	75.0	76	75.5	76	76.1	77.8	76.6
	[IQR]	[22–68]	[65–84]	[69–85]	[66–85]	[72–81]	[71–81]	[72–83]	[72–81]
	Volume (ml)	1603	1601	1575	1604	1591	1590	1584	1588
	[IQR]	[1506–1691]	[1475–1706]	[1462–1670]	[1473–1715]	[1466–1672]	[1468–1666]	[1510–1647]	[1484–1666]
	CDR	0[a]	0	0	0	0.5	0.5	1	0.64
	MMSE	29.0[a]	28.8	28.9	28.8	25.7	25.7	21.7	24.5
	[IQR]	[29–30]	[28–30]	[28–30]	[28–30]	[24–28]	[23–28]	[20 − 23]	[22–28]

		Healthy controls		SCD	MCI	ADD	MCI + ADD
	Matched to	SCD	MCI & ADD	–	–	–	–
UAntwerp Cohort	N	40	24	18	41	34	75
	Sex (M/F)	22/18	12/12	7/11	24/17	15/19	39/36
	Sex (% F)	55	50	39	41	55	48
	Age	63.6	70.3	65.7	71.5	72.1	71.8
	[IQR]	[56–71]	[67–74]	[55–75]	[69–76]	[67–79]	[68–76]
	Volume (ml)	1650	1617	1655	1683	1596	1644
	[IQR]	[1522–1758]	[1492–1723]	[1508–1761]	[1561–1802]	[1505–1675]	[1530–1762]
	MMSE	29.4	29.2	28.5	25.9	20.3	23.4
	[IQR]	[29–30]	[29–30]	[27–30]	[24–27]	[18–24]	[22–26]

With respect to the OASIS database, different subsets were selected to match age and sex in the respective AD groups. Age was matched using a Wilcoxon ranksum test ($p > 0.05$), while sex was matched using a Chi-square test ($p > 0.05$). Volume = estimated Total Intracranial Volume. CDR = Clinical Dementia Rating; MMSE = Mini-Mental State Examination. IQR = Inter Quartile Range.

[a] CDR and MMSE were only available for 130 HCs.

datasets. Significant differences (p-value $< 0.05/3$) are found between matched HCs and the mADD group on both CIR and CCI with a moderate to large effect size. No differences are observed for CCA (Figs. 1 and 2).

In both the OASIS and the Antwerp cohort, CIR was the only feature able to distinguish between HCs and MCI subjects. CIR is also able to distinguish between MCI and mild ADD subjects from the OASIS cohort with a moderate effect size (0.68). Both CIR and CCI were able to discriminate subjects with SCD from HCs with large (0.74) effect sizes.

As we have – for each cohort – defined 3 independent groups, a correction for multiple comparisons across different groups and variables implies a cutoff p-value of $0.05/3/3 = 0.006$. Applying this stricter criterion would not change the results substantially (cf. Table 2).

All features also show a significant correlation with ageing ($p < 0.001$).

3.3. Corpus callosum features vs CSF

Across the whole group, no correlations were observed between CSF markers and callosal features. However, when analyzing the different subgroups independently, the results summarized in Table 3 were obtained. The Bonferroni cutoff for significance was $0.05/15 = 0.003$.

3.4. Thickness profiles

The thickness profile is calculated along 50 equidistantly positioned midline points and compared between the different groups. In order to correct for multiple (=50) comparison problem, while accounting for the inherent correlations of the 50 features, we performed a principal component analysis (PCA). As 11 components explained over 95% of the variance, we estimated the true dimensionality to be 11 (instead of 50). Therefore, a Bonferroni corrected p-value of $0.05/11$ (or $-\log10(\text{pvalue}) > 2.3$) was applied and only streamlines with a $-\log10(\text{p-value}) > 2.3$ are shown.

Fig. 3 shows the differences between mADD subjects and a matched HC cohort. The differences spread out over the genu, the body, the isthmus and the splenium with the most significant differences in the isthmus ($p \sim E-7$). Very few streamlines survive the multiple comparison correction when the other groups are compared (both datasets).

3.5. Correlation with clinical covariates

There are no significant correlations between the different CC features (CCA, CIR and CCI) and MMSE or socio-economic status. By constructing multilinear models consisting of both clinical covariates (age, education and sex) and the length of a single streamline and applying a backward step variable selection procedure based on the Akaike Information Criterion (Akaike, 1974), we could assess which streamlines were significantly retained in models predicting the MMSE and SES. However, none of the streamline lengths survived multiple comparison corrections. Similarly, no significant correlations were found between callosal metrics and MMSE.

3.6. Thickness profile vs CSF biomarker profile

Similar to the summarizing callosal features, no correlations were found between CSF biomarkers and the thickness profile when taking the complete group into account. However, within the SCD group there was a tendency to significance between the thickness in the midcallosal body and tau and Ptau levels ($p < 0.01$) and within the MCI the thickness of the posterior CC correlated with tau and Ptau ($p < 0.001$), see Fig. 4.

Table 2
Comparison of CCA, CIR and CCI.

OASIS						UAntwerp					
HC vs (MCI + mADD)						HC vs (MCI + ADD)					
	P	Cohen's d	Mean HC	Mean MCI & ADD	P-STD		P	Cohen's d	Mean HC	Mean MCI & ADD	P-STD
CCA	0.54	−0.11	3.64	3.69	0.48	CCA	0.050	0.456	3.52	3.32	0.43
CIR	**0.001**	**0.52**	**0.15**	**0.14**	**0.02**	CIR	**7E−4**	**0.796**	**0.17**	**0.15**	**0.03**
CCI	0.022	0.34	0.31	0.30	0.04	CCI	**0.002**	**0.775**	**0.35**	**0.31**	**0.03**
HC vs MCI						HC vs MCI					
	P	Cohen's d	Mean HC	Mean MCI	P-STD		P	Cohen's d	Mean HC	Mean MCI	P-STD
CCA	0.41	−0.15	3.65	3.72	0.50	CCA	0.320	0.326	3.52	3.39	0.39
CIR	0.02	0.39	0.15	0.15	0.02	CIR	**0.009**	**0.699**	**0.17**	**0.15**	**0.03**
CCI	0.12	0.23	0.31	0.31	0.04	CCI	0.023	0.587	0.35	0.32	0.05
HC vs mADD						HC vs ADD					
	P	Cohen's d	Mean HC	Mean ADD	P-STD		P	Cohen's d	Mean HC	Mean ADD	P-STD
CCA	0.70	0.08	3.65	3.61	0.50	CCA	**0.008**	**0.644**	**3.52**	**3.25**	**0.44**
CIR	**4E−5**	**0.96**	**0.15**	**0.13**	**0.02**	CIR	**2E−4**	**0.956**	**0.17**	**0.15**	**0.02**
CCI	**7E−4**	**0.76**	**0.31**	**0.28**	**0.05**	CCI	**7E−4**	**1.045**	**0.35**	**0.31**	**0.04**
MCI vs mADD						HC vs SCD					
	P	Cohen's d	Mean MCI	Mean ADD	P-STD		P	Cohen's d	Mean HC	Mean SCD	P-STD
CCA	0.241	0.25	3.71	3.61	0.42	CCA	0.500	0.357	3.73	3.55	0.49
CIR	**0.004**	**0.68**	**0.14**	**0.13**	**0.02**	CIR	**0.006**	**0.741**	**0.18**	**0.16**	**0.02**
CCI	0.019	0.56	0.30	0.28	0.04	CCI	**0.007**	**0.748**	**0.36**	**0.32**	**0.05**
HC ageing						HC ageing					
	P	r									
CCA	< **0.001**	**−0.51**				CCA	< **0.001**	**−0.54**			
CIR	< **0.001**	**−0.68**				CIR	< **0.001**	**−0.48**			
CCI	< **0.001**	**−0.57**				CCI	< **0.001**	**−0.53**			

p-Values calculated through the Wilcoxon rank test (HC vs pooled AD) and correlation (HC ageing). As effect size, we included Cohen's d effect size obtained in the comparisons HC vs pooled AD and the correlation coefficient r for ageing. All means are dimensionless. CCA: Corpus Callosum Area, CIR: Circularity, CCI: Corpus Callosum Index; P-STD: Pooled standard-deviation.
Bold numbers indicates significance at p-value < 0.05/3 = 0.0167.

3.7. Correlation with normal ageing

Correlations between streamline length and age were calculated using the Pearson correlation coefficient using all healthy controls from the OASIS database. All streamlines correlated significantly with age ($p < E-14$), the explained variance (R^2) is plotted in Fig. 5. In Fig. 5.B we present the CC thickness profile in three different groups divided on age (Age < 40, 40 < Age < 70, Age > 70). As can be seen, minor reductions in thickness can be seen in the rostrum and body in the group of controls aged between 40 and 70.

4. Discussion

In this paper, we have assessed the influence of healthy ageing and AD on the most popular corpus callosum features (CCA, CIR and CCI) and we assessed their relationship with a more detailed thickness profile generated by Laplace's equation. The latter guarantees orthogonal boundary intersections and non-overlapping contours, an important asset when examining neurodegenerative diseases that may induce an increased CC curvature (Adamson et al., 2011).

In the OASIS database, we observed a significant difference in CIR and CCI comparing HCs with mADD and MCI and mADD patients, but no differences in CCA in line with the previously obtained results on the same dataset by Ardekani et al. (2014). Similar findings are observed in the Antwerp dataset with the additional finding of a significantly smaller CCA in the ADD cohort. As the observed significant decrease in CIR (~CCA/Perimeter^2) is not accompanied by a similarly significant decrease in CCA, the callosal perimeter seems to drive the change in CIR indicating an increased curvature.

Interestingly, the Antwerp dataset showed that CIR and CCI were able to distinguish HCs from subjects with SCD ($p \sim 0.006$) with a fairly large effect size (0.75) showing the ability of callosal features to pick up early processes that might be pursued by (Alzheimer's) dementia. The fact that the obtained results are more significant for the HC vs SCD comparison than for the HC vs MCI comparison is likely due to the larger control group that could be included in the HC vs SCD comparison. The observed effect size is larger than the one that can be calculated (assuming a Gaussian distribution) from the results obtained by (Ryu et al., 2017) and similar to (Cantero et al., 2016) (0.64). Ryu found an effect size of 0.17 based on the normalized hippocampal volume, whereas Cantero et al. found effect sizes of 0.64 (Left hippocampus) and 0.53 (Right hippocampus).

In order to illustrate the possible relevance of the obtained results, we ran a classifier that simply applies a cutoff on CIR. This classifier allowed us to discriminate between HCs and SCD subjects with a maximal accuracy of 77% and with a positive predictive value of 75%.

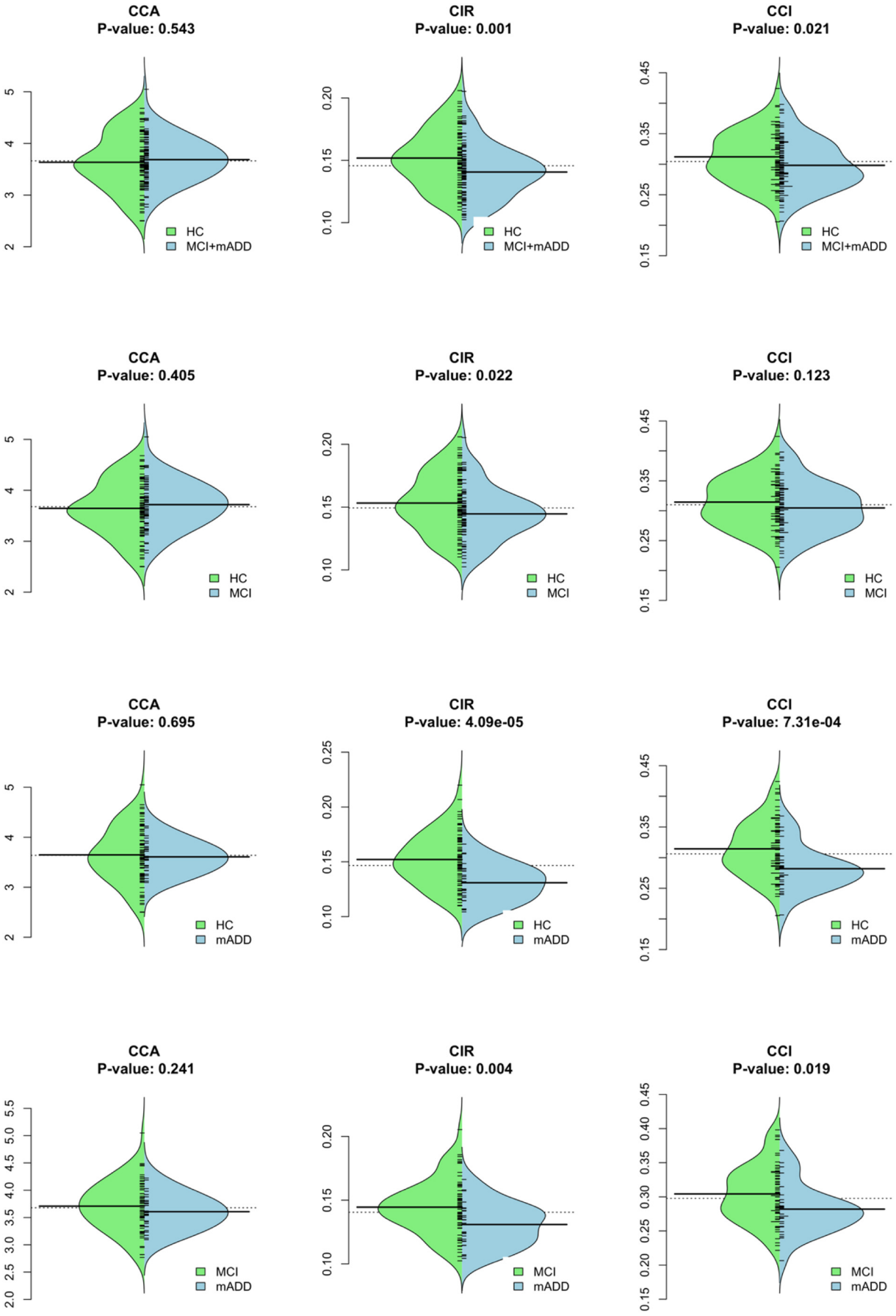

Fig. 1. Beanplot of CCA/CIR/CCI in the different group comparisons for the OASIS dataset.

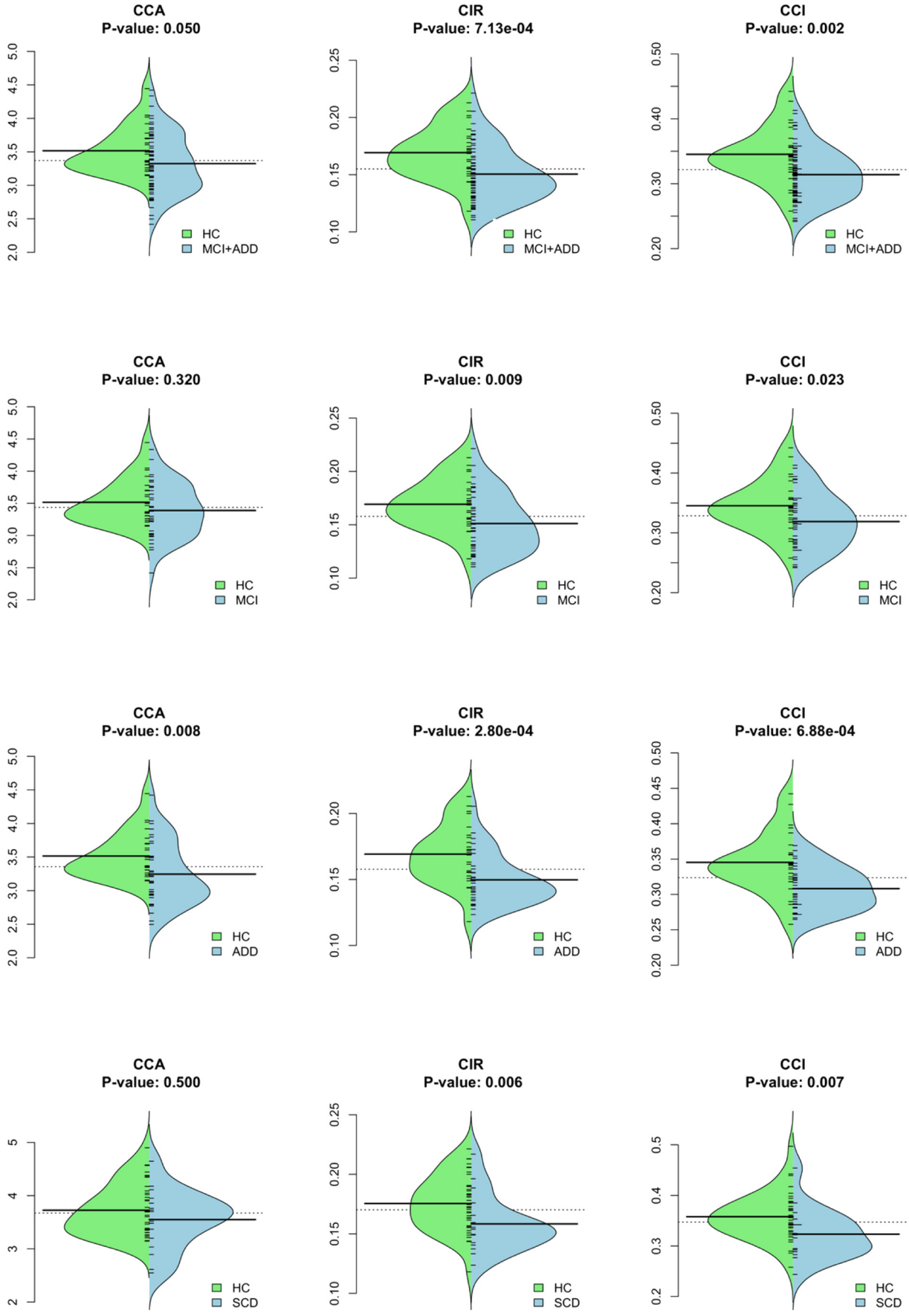

Fig. 2. Beanplots of CCA/CIR/CCI in the different group comparisons for the UAntwerp dataset.

Table 3
p-Values (and Pearson correlation) between the different CSF markers and callosal features obtained in the UAntwerp dataset. No significant correlations were found within the ADD group.

	CCA	CIR	CCI
Subjective cognitive decline			
T-tau	0.88 (0.05)	0.033 (0.59)	0.06 (0.53)
$A\beta_{1-42}$	0.33 (0.30)	0.64 (0.15)	0.13 (0.45)
P-tau_{181}	0.66 (0.14)	**0.005 (0.72)**	**0.008 (0.70)**
Mild cognitive impairment			
T-tau	0.26 (0.18)	**0.002 (0.47)**	**2E−4 (0.55)**
$A\beta_{1-42}$	0.07 (−0.29)	0.18 (−0.21)	0.72 (−0.06)
P-tau_{181}	0.15 (0.23)	**0.007 (0.42)**	**1E−4 (0.56)**

Bold numbers indicates significance at p-value $< 0.05/3/3 = 0.006$.

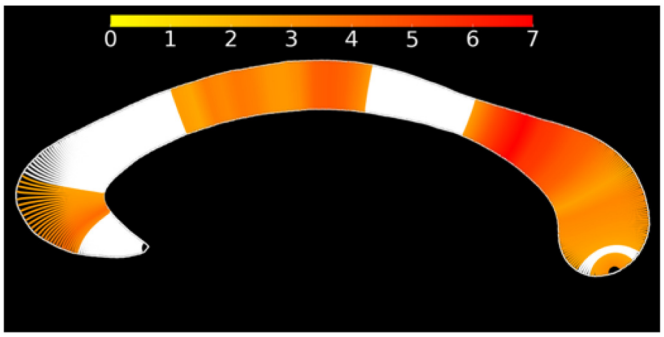

Fig. 3. Results of the comparison between matched healthy controls and mADD patients (OASIS database). Only streamlines that are significantly shorter in the AD group ($p < 0.05/14$) are shown. The largest differences ($p \sim E-7$) can be found in the isthmus. The color encodes the $-\log10(p)$ value obtained through a Wilcoxon ranksum test.

If the goal would be to construct a sensitive sentinel test, i.e. a test that tries to minimize the number of false negatives while retaining a reasonable – but arbitrary – specificity, we obtain a sensitivity of 81% at a specificity of 60%. This finding is important as SCD subjects show greater conversion rates to MCI and dementia due to AD than age-matched HCs (Jessen et al., 2010; Reisberg et al., 2010; van Oijen et al., 2007) and as there is an urgent need to detect and diagnose AD as early as possible.

Whereas the perceived cognitive decline may stem from other causes (rather than being an early stage of AD), there is a consistent evolution of both CIR and CCI across the included spectrum. Both CIR and CCI are largest in the HC group, smallest in the MCI/ADD group and in between for the SCD group.

The observed difference in isthmus thickness in mADD corresponds to the results obtained by Wang et al., who observed a general thinning in the posterior regions (Wang et al., 2006). Yet, Wang et al. additionally observed slightly significant changes between an MCI and a control cohort. On the other hand, Zhu et al. who divided the corpus callosum in 5 sections according to the radial Witelson partition, observed a smaller area of the rostral body and midbody in a cohort of subjects with CDR = 0.5 (Zhu et al., 2012). Although the thickness profile differences between the HC and mADD group may be explained by retrogenesis in the anterior regions and Wallerian degeneration in the posterior regions (Di Paola et al., 2010a, 2010b), results should be treated with caution as the observed did not survive correction for multiple comparison in the Antwerp dataset.

We showed a significant correlation between T-tau and P-tau levels on one hand and CIR/CCI on the other in both the SCD and MCI cohorts, but not in the ADD cohort. A further analysis showed that in the SCD cohort the mid-callosal body thickness correlated with T-tau and P-tau levels, whereas the correlation was maximal in the posterior CC in the MCI cohort. As T-tau levels are CSF biomarkers for neurodegeneration (Niemantsverdriet et al., 2017), these findings suggest that callosal degeneration in SCD mainly affects the callosal midbody, while more posterior regions are affected in the MCI stage. It is important to note that – with respect to the SCD cohort- the correlations are only significant at the $p < 0.01$ level and would not survive correction for multiple testing. Therefore, these results should be interpreted with caution. Correlations between the splenium thickness and P-tau do survive correction for multiple testing in the MCI cohort.

It can be noted that the correlations between T-tau (and P-tau) and CIR/CCI are positive, which is contra-intuitive given the atrophy of the CC with disease progression. Several possible explanations can be hypothesized. One explanation may be that given the proximity of the CC to the lateral ventricles, pathological changes in the CC affect CSF levels more than any other brain structure. In that case, higher levels of CSF T-tau (and P-tau) will be noted in those subjects who still have the largest CC volumes, reflecting more intact CC tissue, prone to neurodegeneration and pathology. Another possible explanation is the idea that the cortical volume may be increased by accumulation of amyloid deposition and the associated inflammatory response (Fortea et al., 2014; Jacobs et al., 2014). This hypothesis was also suggested by (Fox et al., 2005) to explain the lack of effect on MRI of anti-amyloid immunotherapy trials. However, it is important to bear in mind that these analyses were not the primary outcome of this paper and may, therefore, reflect type I errors. It might as well be that these findings have no biological meaning, but rather reflect the heterogeneous nature of the SCD group. More research is warranted to assess this relationship in a

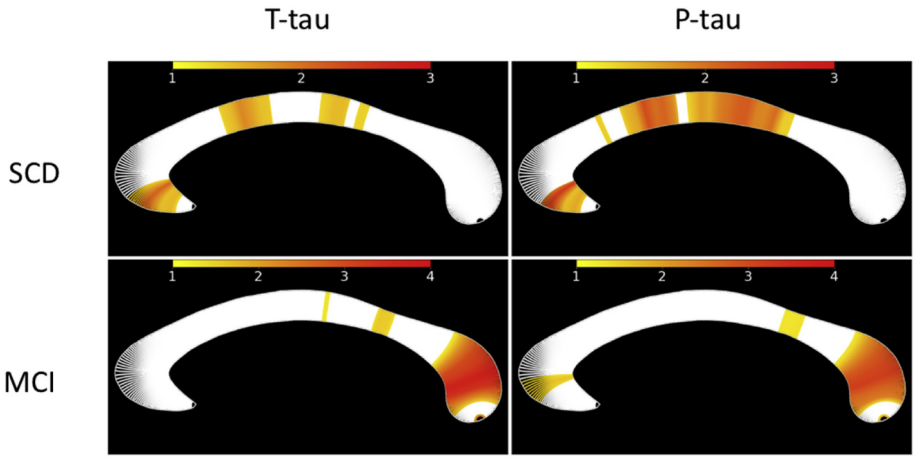

Fig. 4. Correlation between CSF markers T-tau and P-tau and the callosal thickness profile. The color indicates $-\log10$(p-value). Significant streamlines are shown for $p < 0.05$.

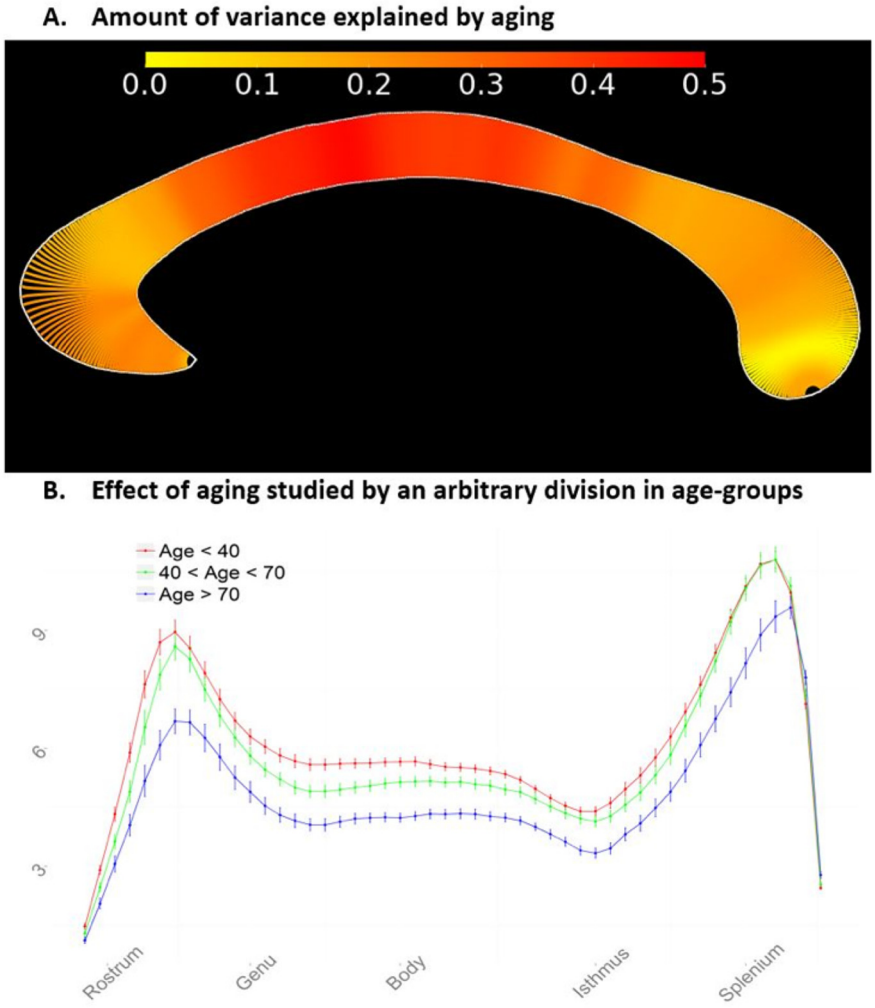

Fig. 5. A. Amount of variance explained by age in a linear model along the Corpus Callosum profile. B. Thickness profile evolution with age subdivided in three arbitrary groups for illustrative purposes only (red: age $<$ 40, N = 149, green: 40 $<$ age $<$ 70, N = 87, blue: age $>$ 70, N = 66). The error bars represent the standard error of the mean in the three age groups. (For interpretation of the references to color in this figure legend, the reader is referred to the web version of this article.)

more detailed (and longitudinal) way.

With respect to normal ageing, we found that with increasing age, CCA, CIR and CCI significantly decline, which corresponds to the findings reported by Ardekani et al. (2014) on the same OASIS database. The thickness profile generation showed that the change in these features is caused by a general decrease in thickness (explained variance varied between 10 and 50%, highest explained variance in the body, only the splenium seems to remain relatively unaffected).

Although our results indicate a uniform thinning of the CC with increasing age, the CC does not thin uniformly at all ages. We observed a significantly thinner anterior CC in the control group between the age of 40 and 70, and a thinner genu and splenium in the group older than 70 years old (Fig. 3).

The rationale for including the callosal thickness profile is the idea that it will enable to provide a more detailed description than the summarizing parameters. Yet, the discriminatory capacity is limited even though summarizing features like CIR and CCI differed significantly (even between SCD and the control cohort) with moderate to large effect sizes for most comparisons.

There are several reasons for which summarizing metrics may be more informative than the more detailed thickness profile: a first one could be a higher reliability and therefore an increased signal-to-noise ratio (Van Schependom et al., 2016); a second one could be the sampling of the thickness profile along 50 equidistance points. Although this procedure was inspired by the literature, it may not be ideal to sample the thickness profile in diseases where the callosal curvature may increase as the length of the midline may also change, obfuscating the straight-forward comparison across patient cohorts.

The main limitation when using the OASIS database is the limited availability of clinical data which only allows to define the clinical subgroups based on the CDR. We overcame this limitation by analyzing an independent dataset including cohorts defined according to the current international standards (cf. Methods). Whereas the diagnosis of all MCI patients was corroborated by a positive CSF or neuroimaging biomarker profile, we did not apply the same restriction on the ADD cohort. The rationale being that the MCI diagnosis is more difficult. Also, nor the UAntwerp nor the OASIS database provided CSF information of healthy controls. This could lead to the inclusion of subthreshold AD patients. Although not ideal, this would only reduce any between-group difference.

Finally, an additional advantage of analyzing two independent cohorts is the possibility to compare results: while there are no large differences when analyzing callosal features, the OASIS database was the only one where the thickness profile showed extensive differences between the mild ADD group and the matched cohort of HCs. This discrepancy might be due to the large statistical power provided by the OASIS database. This statistical power is required to overcome the multiple comparison problem when assessing the thickness profile.

5. Conclusion

To the best of our knowledge, this is the first study investigating changes in corpus callosum features (CCA, CIR and CCI) in normal ageing and AD by exploring both summarizing features and the complete CC thickness profile in two independent cohorts. We showed that features like CIR and CCI significantly differ between HCs and an important subgroup in the early AD spectrum (SCD).

List of abbreviations

CC	corpus callosum
AD	Alzheimer's disease
ADD	Alzheimer's disease dementia
mADD	mild Alzheimer's disease dementia
MCI	mild cognitive impairment
SCD	subjective cognitive decline
HC	healthy controls
CIR	circularity
CCA	callosal area
CCI	corpus callosum index
CDR	Clinical Dementia Rating
MMSE	Mini-Mental State Examination
PCA	principal component analysis
CSF	cerebrospinal fluid
MSP	mid-sagittal plane
MRI	magnetic resonance imaging
$A\beta_{1-42}$	Beta-amyloid 1–42
T-tau	total tau
P-tau_{181}	Tau phosphorylated at threonine 181

Supplementary data to this article can be found online at https://doi.org/10.1016/j.nicl.2018.05.018.

Funding

JVS is supported by a post-doc scholarship by Flanders Research Foundation (FWO, www.fwo.be) (12I1817N). This research was in part funded by the University Research Fund of the University of Antwerp and the Flemish Impulse Financing of Networks for Dementia Research (VIND). The OASIS project was supported by the following NIH grants: P50 AG05681, P01 AG03991, R01 AG021910, P50 MH071616, U24 RR021382, and R01 MH56584.

Author's contributions

JVS, EN, DS and SE were responsible for the conception and design of the study. JVS, EN and SE were responsible for data acquisition, analysis, and interpretation of data. JVS, EN, DS and SE were responsible for drafting the manuscript and revising it critically for important intellectual content. All authors read and approved the final version.

Acknowledgements

The authors acknowledge the assistance of Ellen De Roeck, Naomi De Roeck, Charisse Somers, Hanne Struyfs (BIODEM UAntwerp), and of Peter Mariën, Jos Saerens, and Nore Somers (Department of Neurology and Memory Clinic, Hospital Network Antwerp (ZNA) Middelheim and Hoge Beuken).

References

Adamson, C.L., Wood, A.G., Chen, J., Barton, S., Reutens, D.C., Pantelis, C., Velakoulis, D., Walterfang, M., 2011. Thickness profile generation for the corpus callosum using Laplace's equation. Hum. Brain Mapp. 32, 2131–2140. http://dx.doi.org/10.1002/hbm.21174.

Adamson, C., Beare, R., Walterfang, M., Seal, M., 2014. Software pipeline for midsagittal corpus callosum thickness profile processing: automated segmentation, manual editor, thickness profile generator, group-wise statistical comparison and results display. Neuroinformatics 12, 595–614. http://dx.doi.org/10.1007/s12021-014-9236-3.

Akaike, H.A.I., 1974. A new look at the statistical model identification. IEEE Trans. Autom. Control 19, 716–723.

Akudjedu, T.N., Nabulsi, L., Makelyte, M., Scanlon, C., Hehir, S., Casey, H., Ambati, S., Kenney, J., O'Donoghue, S., Mcdermott, E., Kilmartin, L., Dockery, P., Mcdonald, C., Hallahan, B., Cannon, D.M., 2018. A comparative study of segmentation techniques for the quantification of brain subcortical volume. Brain Imaging Behav. 1, 0. http://dx.doi.org/10.1007/s11682-018-9835-y.

Albert, M.S., DeKosky, S.T., Dickson, D., Dubois, B., Feldman, H.H., Fox, N.C., Gamst, A., Holtzman, D.M., Jagust, W.J., Petersen, R.C., Snyder, P.J., Carrillo, M.C., Thies, B., Phelps, C.H., 2011. The diagnosis of mild cognitive impairment due to Alzheimer's disease: recommendations from the National Institute on Aging-Alzheimer's Association workgroups on diagnostic guidelines for Alzheimer's disease. Alzheimers Dement. 7, 270–279. http://dx.doi.org/10.1016/j.jalz.2011.03.008.

Ardekani, B.A., Figarsky, K., Sidtis, J.J., 2013. Sexual dimorphism in the human corpus callosum: an MRI study using the OASIS brain database. Cereb. Cortex 23, 2514–2520. http://dx.doi.org/10.1093/cercor/bhs253.

Ardekani, B.A., Bachman, A.H., Figarsky, K., Sidtis, J.J., 2014. Corpus callosum shape changes in early Alzheimer's disease: an MRI study using the OASIS brain database. Brain Struct. Funct. 219, 343–352. http://dx.doi.org/10.1007/s00429-013-0503-0.

Boccardi, M., Ganzola, R., Bocchetta, M., Pievani, M., Redolfi, A., Bartzokis, G., Camicioli, R., Csernansky, J.G., de Leon, M.J., DeToledo-Morrell, L., Killiany, R.J., Lehéricy, S., Pantel, J., Pruessner, J.C., Soininen, H., Watson, C., Duchesne, S., Jack, C.R., Frisoni, G.B., 2011. Survey of protocols for the manual segmentation of the hippocampus: preparatory steps towards a joint EADC-ADNI harmonized protocol. J. Alzheimers Dis. 26, 61–75. http://dx.doi.org/10.3233/JAD-2011-0004.Survey.

Cantero, J.L., Iglesias, J.E., Van Leemput, K., Atienza, M., 2016. Regional hippocampal atrophy and higher levels of plasma amyloid-beta are associated with subjective memory complaints in nondemented elderly subjects. J. Gerontol. A Biol. Sci. Med. Sci. 71, 1210–1215. http://dx.doi.org/10.1093/gerona/glw022.

Di Paola, M., Di Iulio, F., Cherubini, A., Blundo, C., Casini, A.R., Sancesario, G., Passafiume, D., Caltagirone, C., Spalletta, G., 2010a. When, where, and how the corpus callosum changes in MCI and AD: a multimodal MRI study. Neurology 74, 1136–1142. http://dx.doi.org/10.1212/WNL.0b013e3181d7d8cb.

Di Paola, M., Luders, E., Di Iulio, F., Cherubini, A., Passafiume, D., Thompson, P.M., Caltagirone, C., Toga, A.W., Spalletta, G., 2010b. Callosal atrophy in mild cognitive impairment and Alzheimer's disease: different effects in different stages. NeuroImage 49, 141–149. http://dx.doi.org/10.1016/j.neuroimage.2009.07.050.

Dubois, B., Feldman, H.H., Jacova, C., Hampel, H., Molinuevo, J.L., Blennow, K., Dekosky, S.T., Gauthier, S., Selkoe, D., Bateman, R., Cappa, S., Crutch, S., Engelborghs, S., Frisoni, G.B., Fox, N.C., Galasko, D., Habert, M.O., Jicha, G.A., Nordberg, A., Pasquier, F., Rabinovici, G., Robert, P., Rowe, C., Salloway, S., Sarazin, M., Epelbaum, S., de Souza, L.C., Vellas, B., Visser, P.J., Schneider, L., Stern, Y., Scheltens, P., Cummings, J.L., 2014. Advancing research diagnostic criteria for Alzheimer's disease: the IWG-2 criteria. Lancet Neurol. 13, 614–629. http://dx.doi.org/10.1016/S1474-4422(14)70090-0.

Filippi, M., Agosta, F., Frisoni, G.B., De Stefano, N., Bizzi, A., Bozzali, M., Falini, A., Rocca, M.A., Sorbi, S., Caltagirone, C., Tedeschi, G., 2012. Magnetic resonance imaging in Alzheimer's disease: from diagnosis to monitoring treatment effect. Curr. Alzheimer Res. 9, 1198–1209.

Folstein, M., Folstein, S., McHugh, P., 1975. Mini-mental state: a practical method for grading the cognitive state of patients for the clinician. J. Psychiatr. Res. 12, 189–198.

Fortea, J., Vilaplana, E., Alcolea, D., Carmona-Iragui, M., Sala, I., González, S., Medrano, S., Pegueroles, J., Morenas, E., Clarimon, J., Blesa, R., Lleo, A., (ADNI), A.D.N.I, 2014. CSF β-amyloid and phospho-tau biomarker interactions on brain structure in preclinical AD. Ann. Neurol. 2–31. http://dx.doi.org/10.1002/acr.22212.

Fox, N.C., Black, R.S., Gilman, S., Rossor, M.N., Griffith, S.G., Jenkins, L., Koller, M., 2005. Effects of Abeta immunization (AN1792) on MRI measures of cerebral volume in Alzheimer disease. Neurology 64, 1563–1572. http://dx.doi.org/10.1212/01.WNL.0000159743.08996.99.

Frederiksen, K.S., Garde, E., Skimminge, A., Ryberg, C., Rostrup, E., Baaré, W.F.C., Siebner, H.R., Hejl, A.M., Leffers, A.M., Waldemar, G., 2011. Corpus callosum atrophy in patients with mild Alzheimer's disease. Neurodegener. Dis. 476–482. http://dx.doi.org/10.1159/000327753.

Frisoni, G.B., Fox, N.C., Jack Jr., C.R., Scheltens, P., Thompson, P.M., 2010. The clinical use of structural MRI in Alzheimer disease. Nat. Rev. Neurol. 6, 67–77. http://dx.doi.org/10.1016/j.neurobiolaging.2008.06.016.

Hampel, H., Teipel, S.J., Alexander, G.E., Horwitz, B., Teichberg, D., Schapiro, M.B., Rapoport, S.I., 1998. Corpus callosum atrophy is a possible Indicator of region– and cell type–specific neuronal degeneration in Alzheimer disease. Arch. Neurol. 55, 193–198. http://dx.doi.org/10.1001/archneur.55.2.193.

Hampel, H., Teipel, S.J., Alexander, G.E., Pogarell, O., Rapoport, S.I., Möller, H.J., 2002. In vivo imaging of region and cell type specific neocortical neurodegeneration in Alzheimer's disease: perspectives of MRI derived corpus callosum measurement for mapping disease progression and effects of therapy. Evidence from studies with MRI, EEG and. J. Neural Transm. 109, 837–855. http://dx.doi.org/10.1007/s007020200069.

Jack, C.R., Albert, M.S., Knopman, D.S., McKhann, G.M., Sperling, R.A., Carrillo, M.C., Thies, B., Phelps, C.H., 2011. Introduction to the recommendations from the National Institute on Aging-Alzheimer's Association workgroups on diagnostic guidelines for Alzheimer's disease. Alzheimers Dement. 7, 257–262. http://dx.doi.org/10.1016/j.

jalz.2011.03.004.
Jacobs, H.I., Clerx, L., Gronenschild, E.H., Aalten, P., Verhey, F.R., 2014. White matter hyperintensities are positively associated with cortical thickness in Alzheimer's disease. J. Alzheimers Dis. 39, 409–422. http://dx.doi.org/10.3233/JAD-131232.
Jessen, F., Wiese, B., Bachmann, C., Eifflaender-Gorfer, S., Haller, F., Kölsch, H., Luck, T., Mösch, E., Van Den Bussche, H., Wagner, M., Wollny, A., Zimmermann, T., Pentzek, M., Riedel-Heller, S.G., Romberg, H.P., Weyerer, S., Kaduszkiewicz, H., Maier, W., Bickel, H., 2010. Prediction of dementia by subjective memory impairment effects of severity and temporal association with cognitive impairment. Arch. Gen. Psychiatry 67, 414–422. http://dx.doi.org/10.1001/archgenpsychiatry.2010.30.
Jessen, F., Amariglio, R.E., Van Boxtel, M., Breteler, M., Dubois, B., Dufouil, C., Ellis, K.A., Flier, W.M., Van Der Glodzik, L., Van Harten, A.C., De Leon, M.J., Mchugh, P., Mielke, M.M., Luis, J., Mosconi, L., Osorio, R.S., Perrotin, A., Petersen, R.C., Rabin, L.A., Rami, L., Reisberg, B., Rentz, D.M., Sachdev, P.S., De, V., Saykin, A.J., Scheltens, P., Shulman, M.B., Slavin, M.J., Sperling, R.A., Stewart, R., Uspenskaya, O., Vellas, B., Jelle, P., Wagner, M., Cognitive, S., Initiative, D., Group, S.W., 2014. A conceptual framework for research on subjective cognitive decline in preclinical Alzheimer's disease. Alzheimers Dement. 10, 844–852. http://dx.doi.org/10.1016/j.jalz.2014.01.001.
Kennedy, K.M., Erickson, K.L., Rodrigue, K.M., Voss, M.W., Colcombe, S.J., Kramer, A.F., Acker, J.D., Raz, N., 2010. Age-related differences in regional brain volumes: a comparison of optimized voxel-based morphometry to manual volumetry. Neurobiol. Aging 30, 1657–1676. http://dx.doi.org/10.1016/j.neurobiolaging.2007.12.020. Age-related.
Luders, E., Narr, K.L., Bilder, R.M., Thompson, P.M., Szeszko, P.R., Hamilton, L., Toga, A.W., 2007. Positive correlations between corpus callosum thickness and intelligence. NeuroImage 37, 1457–1464. http://dx.doi.org/10.1016/j.neuroimage.2007.06.028.
Lyoo, I.K., Satlin, A., Lee, C.K., Renshaw, P.F., 1997. Regional atrophy of the corpus callosum in subjects with Alzheimer's disease and multi-infarct dementia. Psychiatry Res. Neuroimaging 74, 63–72. http://dx.doi.org/10.1016/S0925-4927(97)00009-7.
Marcus, D.S., Wang, T.H., Parker, J., Csernansky, J.G., Morris, J.C., Buckner, R.L., 2007. Open access series of imaging studies (OASIS): cross-sectional MRI data in young, middle aged, nondemented, and demented older adults. J. Cogn. Neurosci. 19, 1498–1507.
McKhann, G.M., Knopman, D.S., Chertkow, H., Hyman, B.T., Jack, C.R., Kawas, C.H., Klunk, W.E., Koroshetz, W.J., Manly, J.J., Mayeux, R., Mohs, R.C., Morris, J.C., Rossor, M.N., Scheltens, P., Carrillo, M.C., Thies, B., Weintraub, S., Phelps, C.H., 2011. The diagnosis of dementia due to Alzheimer's disease: recommendations from the National Institute on Aging-Alzheimer's Association workgroups on diagnostic guidelines for Alzheimer's disease. Alzheimers Dement. 7, 263–269. http://dx.doi.org/10.1016/j.jalz.2011.03.005.
Morris, J.C., 1993. The clinical dementia rating (CDR): current version and scoring rules. Neurology 43, 2412–2414. http://dx.doi.org/10.1212/WNL.43.11.2412-a.
Morris, J.C., Storandt, M., Miller, J.P., McKeel, D.W., Price, J.L., Rubin, E.H., Berg, L., 2001. Mild cognitive impairment represents early-stage Alzheimer disease. Arch. Neurol. 58, 397–405. http://dx.doi.org/10.1001/archneur.58.3.397.
Niemantsverdriet, E., Valckx, S., Bjerke, M., Engelborghs, S., 2017. Alzheimer's disease CSF biomarkers: clinical indications and rational use. Acta Neurol. Belg. 117 (3), 591–602.
Ortiz Alonso, T., Martinez Castillo, E., Fernandez, L.A., Arranzola Garcia, J., Maestu Unturbe, F., Lopez-Ibor, J., 2000. Callosal atrophy and associated electromyographic responses in Alzheimer's disease and aging. Electromyogr. Clin. Neurophysiol. 40, 465–475.
Plassard, A.J., McHugo, M., Heckers, S., Landmann, B.A., 2017. Multi-scale hippocampal parcellation improves atlas-based segmentation accuracy Andrew. Proc. SPIE Int. Soc. Opt. Eng. http://dx.doi.org/10.1016/j.pediatrneurol.2015.01.016.Pathophysiology.
Reisberg, B., Shulman, M.B., Torossian, C., Leng, L., Zhu, W., 2010. Outcome over seven years of healthy adults with and without subjective cognitive impairment. Alzheimers Dement. 6, 11–24. http://dx.doi.org/10.1016/j.jalz.2009.10.002.
Rubin, E.H., Storandt, M., Miller, J.P., Kinscherf, D.A., Grant, E.A., Morris, J.C., Berg, L., 1998. A prospective study of cognitive function and onset of dementia in cognitively healthy elders. Arch. Neurol. 55, 395–401. http://dx.doi.org/10.1001/archneur.55.3.395.
Ryu, S.Y., Lim, E.Y., Na, S., Shim, Y.S., Cho, J.H., Yoon, B., Hong, Y.J., Yang, D.W., 2017. Hippocampal and entorhinal structures in subjective memory impairment: a combined MRI volumetric and DTI study. Int. Psychogeriatr. 29, 785–792. http://dx.doi.org/10.1017/S1041610216002349.
Scheltens, P., Leys, D., Barkhof, F., Huglo, D., Weinstein, H., Vermersch, P., Kuiper, M., Steinling, M., Wolters, E.C., Valk, J., 1992. Atrophy of medial temporal lobes on MRI in “probable” Alzheimer's disease and normal ageing: diagnostic value and neuropsychological correlates: table 1. J. Neurol. Neurosurg. Psychiatry 55, 967–972. http://dx.doi.org/10.1136/jnnp-2012-302562.
Sperling, R.A., Aisen, P.S., Beckett, L.A., Bennett, D.A., Craft, S., Fagan, A.M., Iwatsubo, T., Jack, C.R., Kaye, J., Montine, T.J., Park, D.C., Reiman, E.M., Rowe, C.C., Siemers, E., Stern, Y., Yaffe, K., Carrillo, M.C., Thies, B., Morrison-Bogorad, M., Wagster, M.V., Phelps, C.H., 2011. Toward defining the preclinical stages of Alzheimer's disease: recommendations from the National Institute on Aging-Alzheimer's Association workgroups on diagnostic guidelines for Alzheimer's disease. Alzheimers Dement. 7, 280–292. http://dx.doi.org/10.1016/j.jalz.2011.03.003.
Teipel, S.J., Hampel, H., Alexander, G.E., Schapiro, M.B., Horwitz, B., Teichberg, D., Daley, E., Hippius, H., Möller, H.J., Rapoport, S.I., 1998. Dissociation between corpus callosum atrophy and white matter pathology in Alzheimer's disease. Neurology 51 (5), 1381. http://dx.doi.org/10.1212/WNL.51.5.1381.
Teipel, S.J., Hampel, H., Pietrini, P., Alexander, G.E., Horwitz, B., Daley, E., Moller, H.J., Schapiro, M.B., Rapoport, S.I., 1999. Region-specific corpus callosum atrophy correlates with the regional pattern of cortical glucose metabolism in Alzheimer disease. Arch. Neurol. 56, 467–473. http://dx.doi.org/10.1001/archneur.56.4.467.
Teipel, S.J., Bayer, W., Alexander, G.E., Zebuhr, Y., Teichberg, D., Kulic, L., Schapiro, M.B., Möller, H.-J., Rapoport, S.I., Hampel, H., 2002. Progression of corpus callosum atrophy in Alzheimer disease. Arch. Neurol. 59, 243–248. http://dx.doi.org/10.1001/archneur.59.2.243.
Thompson, P.M., Moussai, J., Zohoori, S., Goldkorn, A., Khan, A.A., Mega, M.S., Small, G.W., 1998. Cortical variablity and asymmetry in normal aging and Alzheimer's disease. Cereb. Cortex 8, 492–509.
Tomaiuolo, F., Scapin, M., Di Paola, M., Le Nezet, P., Fadda, L., Musicco, M., Caltagirone, C., Collins, D.L., 2007. Gross anatomy of the corpus callosum in Alzheimer's disease: regions of degeneration and their neuropsychological correlates. Dement. Geriatr. Cogn. Disord. 23, 96–103. http://dx.doi.org/10.1159/000097371.
Van Der Mussele, S., Fransen, E., Struyfs, H., Luyckx, J., Mariën, P., Saerens, J., Somers, N., Goeman, J., De Deyn, P.P., Engelborghs, S., 2014. Depression in mild cognitive impairment is associated with progression to alzheimer's disease: a longitudinal study. J. Alzheimers Dis. 42, 1239–1250. http://dx.doi.org/10.3233/JAD-140405.
van Oijen, M., de Jong, F.J., Hofman, A., Koudstaal, P.J., Breteler, M.M.B., 2007. Subjective memory complaints, education, and risk of Alzheimer's disease. Alzheimers Dement. 3, 92–97. http://dx.doi.org/10.1016/j.jalz.2007.01.011.
Van Schependom, J., Jain, S., Cambron, M., Vanbinst, A.-M., De Mey, J., Smeets, D., Nagels, G., 2016. Reliability of measuring regional callosal atrophy in neurodegenerative diseases. Neuroimage Clin. 825–831. http://dx.doi.org/10.1016/j.nicl.2016.10.012. (October).
Van Schependom, J., Gielen, J., Laton, J., Sotiropoulos, G., Vanbinst, A., De Mey, J., Smeets, D., Nagels, G., 2017. The effect of morphological and microstructural integrity of the corpus callosum on cognition, fatigue and depression in mildly disabled MS patients. Magn. Reson. Imaging 40, 109–114. http://dx.doi.org/10.1016/j.mri.2017.04.010.
Wang, H., Su, M.Y., 2006. Regional pattern of increased water diffusivity in hippocampus and corpus callosum in mild cognitive impairment. Dement. Geriatr. Cogn. Disord. 22, 223–229. http://dx.doi.org/10.1159/000094934.
Wang, P.J., Saykin, A.J., Flashman, L.A., Wishart, H.A., Rabin, L.A., Santulli, R.B., McHugh, T.L., MacDonald, J.W., Mamourian, A.C., 2006. Regionally specific atrophy of the corpus callosum in AD, MCI and cognitive complaints. Neurobiol. Aging 27, 1613–1617. http://dx.doi.org/10.1016/j.neurobiolaging.2005.09.035.
Yaldizli, Ö., Penner, I.-K., Frontzek, K., Naegelin, Y., Amann, M., Papadopoulou, A., Sprenger, T., Kuhle, J., Calabrese, P., Radü, E.W., Kappos, L., Gass, A., Yaldizli, O., Penner, I.-K., Frontzek, K., Naegelin, Y., Amann, M., Papadopoulou, A., Sprenger, T., Kuhle, J., Calabrese, P., Radü, E.W., Kappos, L., Gass, A., 2013. The relationship between total and regional corpus callosum atrophy, cognitive impairment and fatigue in multiple sclerosis patients. Mult. Scler. J. 20, 356–364. http://dx.doi.org/10.1177/1352458513496880.
Yamauchi, H., Fukuyama, H., Nagahama, Y., Katsumi, Y., Hayashi, T., Oyanagi, C., Konishi, J., Shio, H., 2000. Comparison of the pattern of atrophy of the corpus callosum in frontotemporal dementia, progressive supranuclear palsy, and Alzheimer's disease. J. Neurol. Neurosurg. Psychiatry 69, 623–629. http://dx.doi.org/10.1136/jnnp.69.5.623.
Zandifar, A., Fonov, V., Coupé, P., Pruessner, J., Collins, D.L., 2017. A comparison of accurate automatic hippocampal segmentation methods. NeuroImage 155, 383–393. http://dx.doi.org/10.1016/j.neuroimage.2017.04.018.
Zhu, M., Gao, W., Wang, X., Shi, C., Lin, Z., 2012. Progression of corpus callosum atrophy in early stage of Alzheimer's disease. MRI based study. Acad. Radiol. 19, 512–517. http://dx.doi.org/10.1016/j.acra.2012.01.006.